

Phased array inspection of large size forged steel parts

Frederic Dupont-Marillia, Mohammad Jahazi, and Pierre Belanger

Citation: [AIP Conference Proceedings](#) **1949**, 080004 (2018); doi: 10.1063/1.5031561

View online: <https://doi.org/10.1063/1.5031561>

View Table of Contents: <http://aip.scitation.org/toc/apc/1949/1>

Published by the [American Institute of Physics](#)

Articles you may be interested in

[Influence of local mechanical properties of high strength steel from large size forged ingot on ultrasonic wave velocities](#)

[AIP Conference Proceedings](#) **1806**, 090002 (2017); 10.1063/1.4974646

[Sensitivity images for multi-view ultrasonic array inspection](#)

[AIP Conference Proceedings](#) **1949**, 080001 (2018); 10.1063/1.5031558

[Blending of phased array data](#)

[AIP Conference Proceedings](#) **1949**, 080005 (2018); 10.1063/1.5031562

[Full matrix capture and the total focusing imaging algorithm using laser induced ultrasonic phased arrays](#)

[AIP Conference Proceedings](#) **1806**, 020022 (2017); 10.1063/1.4974563

[ULTRASONIC PHASED ARRAY INSPECTION OF FLAWS ON WELD FUSION FACES USING FULL MATRIX CAPTURE](#)

[AIP Conference Proceedings](#) **1096**, 848 (2009); 10.1063/1.3114345

[Ultrasound beam characteristics of a symmetric nodal origami based array](#)

[AIP Conference Proceedings](#) **1949**, 080006 (2018); 10.1063/1.5031563

Phased Array Inspection Of Large Size Forged Steel Parts

Frederic Dupont-Marillia^{1,a)}, Mohammad Jahazi^{1,b)}, Pierre Belanger^{1,c)}

¹ *Department of mechanical engineering, École de technologie supérieure, Montreal, Quebec, Canada*

^{a)}Corresponding author: frederic.dupont.1@ens.etsmtl.ca

^{b)}mohammad.jahazi@etsmtl.ca

^{c)}pierre.belanger@etsmtl.ca

Abstract. High strength forged steel requires uncompromising quality to warrant advance performance for numerous critical applications. Ultrasonic inspection is commonly used in nondestructive testing to detect cracks and other defects. In steel blocks of relatively small dimensions (at least two directions not exceeding a few centimetres), phased array inspection is a trusted method to generate images of the inside of the blocks and therefore identify and size defects. However, casting of large size forged ingots introduces changes of mechanical parameters such as grain size, the Young's modulus, the Poisson's ratio, and the chemical composition. These heterogeneities affect the wave propagation, and consequently, the reliability of ultrasonic inspection and the imaging capabilities for these blocks. In this context, a custom phased array transducer designed for a 40-ton bainitic forged ingot was investigated. Following a previous study that provided local mechanical parameters for a similar block, two-dimensional simulations were made to compute the optimal transducer parameters including the pitch, width and number of elements. It appeared that depending on the number of elements, backwall reconstruction can generate high amplitude artefacts. Indeed, the large dimensions of the simulated block introduce numerous constructive interferences from backwall reflections which may lead to important artefacts. To increase image quality, the reconstruction algorithm was adapted and promising results were observed and compared with the scattering cone filter method available in the CIVA software.

INTRODUCTION

High strength forged steel is commonly used in many industrial applications like injection molding for automotive bodywork, pipes in oil and gas industries or mining extracting tools. The assessment of the material quality requires extensive nondestructive evaluation (NDE). Ultrasonic testing is a well-known nondestructive technique widely used for crack and heterogeneity detection. Indeed, this technology allows the detection and sizing of defects by studying the propagation of ultrasounds inside the test sample. When the wave encounters a change of acoustic impedance, a part of its energy is reflected and an echo is generated that indicates a feature or a defect. Thanks to the new technologies and miniaturization, more complex ultrasound inspection methods have been developed such as phased array imaging[1]. Based on the same principle of wave reflection, this technique combines an array of emitters and receptors controlled by acquisition sequences. The result is usually given as a B-Scan that can also be post-processed with imaging algorithms like Total Focusing Method (TFM)[2], synthetic aperture focusing technique (SAFT)[3] or MUltiple SIGnal Classification (MUSIC)[4-5] to generate images that are easier to interpret. Phased array imaging is nowadays commonly used in numerous industries. This paper is defined in this context and aims to study phased array inspection possibilities of large size (more than 1 metre in each direction) forged steel parts. Indeed the large dimensions introduce various problems like material heterogeneities, high attenuation and imaging artefacts.

This work leveraged results from a previous study that provided metallurgical information for a high strength large size forged steel block [6]. A model was made using the CIVA Extende software to optimize the design parameters of a custom phased array transducer aiming at inspecting a 1000 mm forged steel block. Also, an algorithm for minimizing artefacts that appear in the particular case of large part dimensions is proposed. The paper begins by a presentation of the material and the simulation model, then results and optimizations are presented and discussed, and finally conclusions are drawn.

MATERIAL AND METHODS

Material

A 40-ton bainitic steel ingot that was forged and heat treated was used in this study. This work was based on a previous ultrasonic study [7] that provided metallurgical and ultrasonic wave propagation properties for this particular material. As the dimensions of the block were more than 1 m in all directions, its casting was hard to control and by extension so were the mechanical parameters. Indeed, the cooling time was more than 14 hours during which the internal flows were not frozen and lead to chemical heterogeneities, macro segregation and Young's modulus variations. Also during heat treatments, including tempering and quenching, core temperature remains higher than the surface temperature for a significantly longer time, leading to grain growth at the core. Measurements showed that grain size was varying from 700 μm at the core of the ingot to 70 μm near the surface. From an ultrasound wave propagation study, it was observed that the material had low dispersion and group wave velocities were mainly affected by the Young's modulus, and local chemical composition was correlated with the density. Finally, velocity measurements along the inspection axis varied by only 5 m/s representing a 0.85% uncertainty on the Time of Flight (TOF). Attenuation was also measured at 0.11 dB/mm at 2 MHz, which is coherent with literature[8].

Method

In order to compute the optimal transducer parameters for the phased array probe, a model was made with the CIVA simulating platform and included 375 cases using the variation module. The block dimensions for this simulation were 1000 mm in every direction, and calculations were made in two dimensions for computing time reasons. In order to observe the response of a 1.587 mm diameter defect at different depths, five simulations were made with the distance between the top surface of the block and the defect varying from 50 mm to 900 mm. The material was taken as close as possible to the results from the ultrasound propagation study. However the velocity variation along the inspection axis was not considered because it was less than 1%. Longitudinal and shear wave velocities were respectively set to 3050 m/s, and 5940 m/s and attenuation was defined using:

$$\alpha(f) = \sum_{p=1}^n \alpha_p f^p \quad (1)$$

with α_0 the attenuation value measured at the frequency f_0 , f the frequency and p is the power of the frequency. Based on measurements, simulations in the present study were performed with $\alpha_0 = 0.11$ dB/mm, $f_0 = 2$ MHz and $p = 2$.

Considering the dimensions of the block under inspection, the main concern was the attenuation associated with the long propagation distances. For this reason, the inspection frequency was set at 2.25 MHz with an 80 % bandwidth as commonly used for large steel blocks. The inspection angle was chosen to be along the vertical axis without any angled wedge in order to reduce as much as possible the traveled distances. To cover the maximum possibilities, the element width varied from 1 mm to 20 mm and the number of elements was set to 8, 16, 32, 64 and 128. The pitch was limited to 1 mm. This limit is related to our 3D printing capabilities so as to fabricate a prototype of the probe. Element length was not considered because simulations were made in two dimensions. Full Matrix Capture (FMC)[9] acquisition sequences were used to produce images using the Total Focusing Method (TFM)[10].

Three parameters were extracted from the images: (1) the amplitude of the defect in the image, (2) the lateral resolution and (3) the vertical resolution. Resolutions were determined using the distance within which the amplitude was greater than -6 dB relative to the defect maximum.

RESULTS AND DISCUSSION

Amplitude and Resolution Optimization

Results extracted from TFM images are provided for 16, 64 and 128 elements and as a function of element widths. Amplitudes below -80 dB and resolution above 50 mm were removed. First, the amplitude is presented:

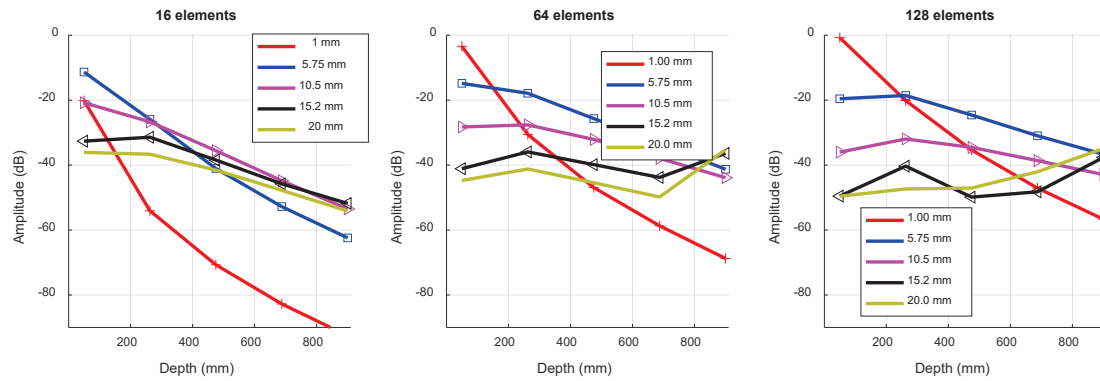


FIGURE 1. Defect amplitude after TFM reconstruction as a function of the element width and the defect depth.

As it is possible to observe in Fig. 1, the case where the element width was 1 mm was highly attenuated over the depth. This result confirmed that commercial probes are not adapted to the inspection of large size forged steel blocks. Increasing the element width reduces the amplitude at low depth but also reduces the averaged amplitudes. Therefore, for element width of 5.75 mm, 10.5 mm, 15.2 mm or 20.0 mm, the amplitude at high depth remains roughly constant.

The lateral resolutions as a function of depth, element width and the number of elements are presented in Fig. 2.

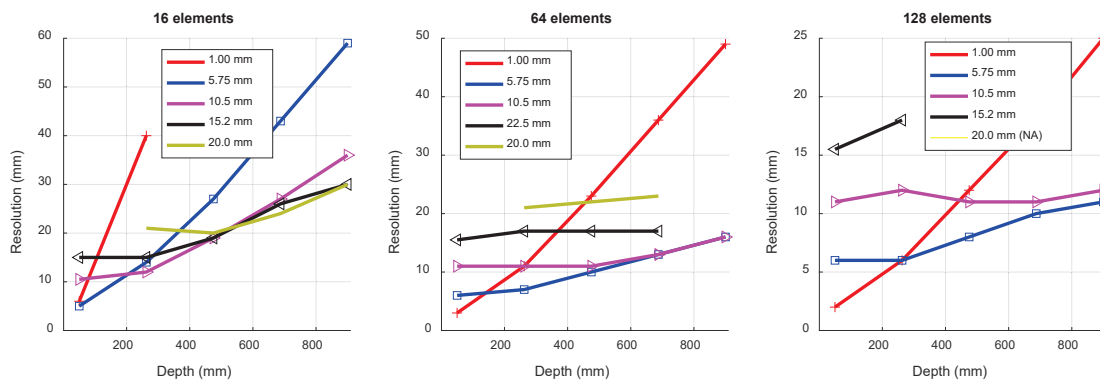


FIGURE 2. Lateral resolution of defect TFM reconstruction as a function of the element width and the defect depth.

The lateral resolution was varying from 5 mm to values higher than 50 mm. This parameter appeared to be an important limitation. Narrow elements, *e.g.*, 1 mm width, are not adapted for inspections for distances above 400 mm. The element number also affects resolution, and some 128 element cases appeared to provide resolution higher than 50 mm because of artefacts introduced in the images that will be discussed in the following section.

Finally, the vertical resolutions as a function of depth, element width and the number of elements are presented in Fig. 3.

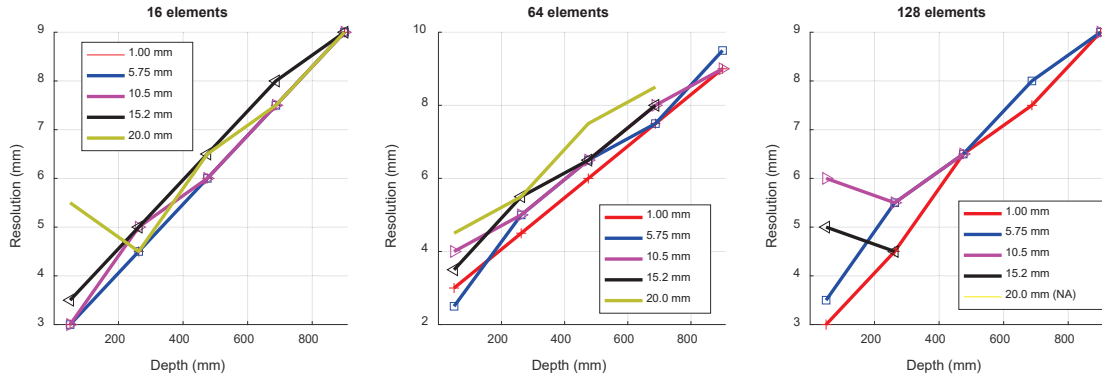


FIGURE 3. Vertical resolution of defect TFM reconstruction as a function of the element width and the defect depth.

The vertical resolutions were relatively low compared to the lateral resolution. For this reason, this parameter was not the main concern for the phased array transducer design. The results suggest that the element width has a low impact on the vertical resolution. When studying the amplitude and the resolution, it appeared that standard transducers could not be used to perform inspection of blocks larger than 400 mm. It was observed that the amplitude criterion leads to element widths of at least 5 mm, vertical resolution remains between 3 mm and 10 mm, but the main limitation was the lateral resolution. From the reconstructed amplitude and the resolution calculation, it also appeared that the best configuration would provide an amplitude loss of 18 dB at a defect at 400 mm depth when considering the backwall reflection as the reference. The vertical and lateral resolutions would respectively be 5.5 mm and 25 mm. Also, for 128 elements of 20 mm the lateral resolution was higher than 50 mm due to the artefacts deteriorating the images. The reconstructed images are presented in Fig. 4 for a defect at 262.5 mm in a 1000 mm block for a 128 element transducer with two different element widths.

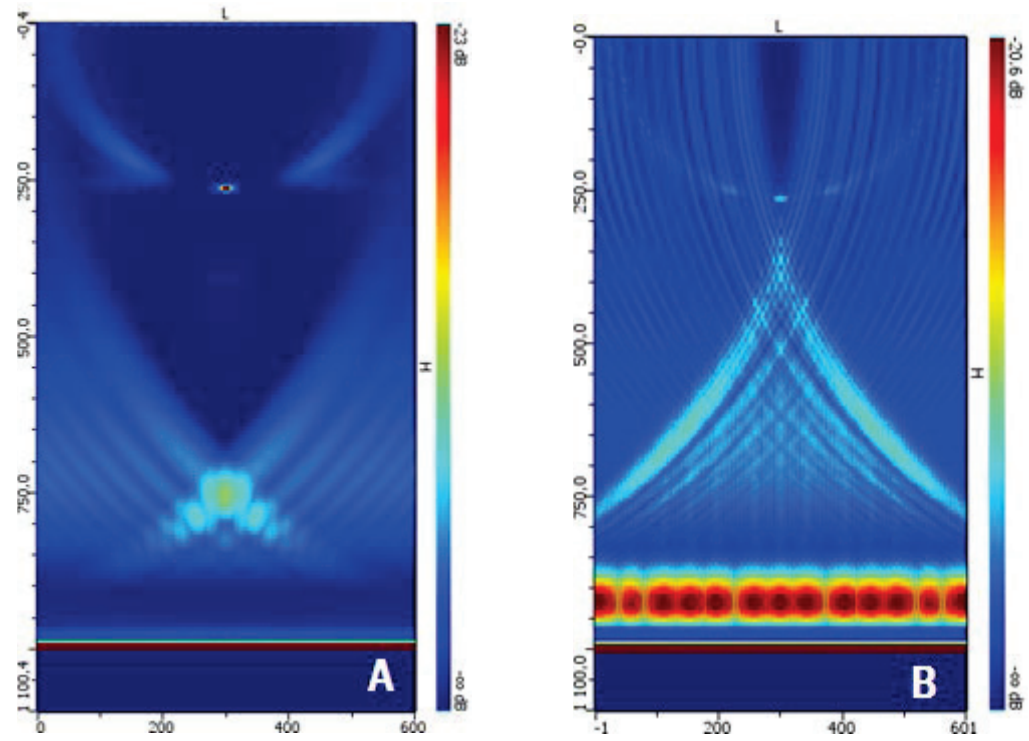


FIGURE 4. Imaging artefacts for 262.5mm depth defect in a large size forged steel for 2 element width: 5.75mm (A), 20mm (B).

In order to increase the transducer design possibilities to allow the use of more elements and increase their size, artefacts suppression is proposed.

Artefacts Suppression

The artefacts were associated to backwall reflections in the case of 64 and 128 elements of at least 10 mm width. This limitation was a strong concern for the transducer design because it limited amplitude and resolution for deep inspection by limiting the element count and dimensions. First, the scattering cone filter, a TFM algorithm implemented in the CIVA software was applied. It selects contributions from an angular sector for which the arrival angle of the path to the element is included and it ignores the rest of the contributions. Artefacts removing on TFM images using the scattering cone filter were computed for arrival angles of 40° , 30° and 20° . The results were compared with standard TFM and are presented in Fig. 5.

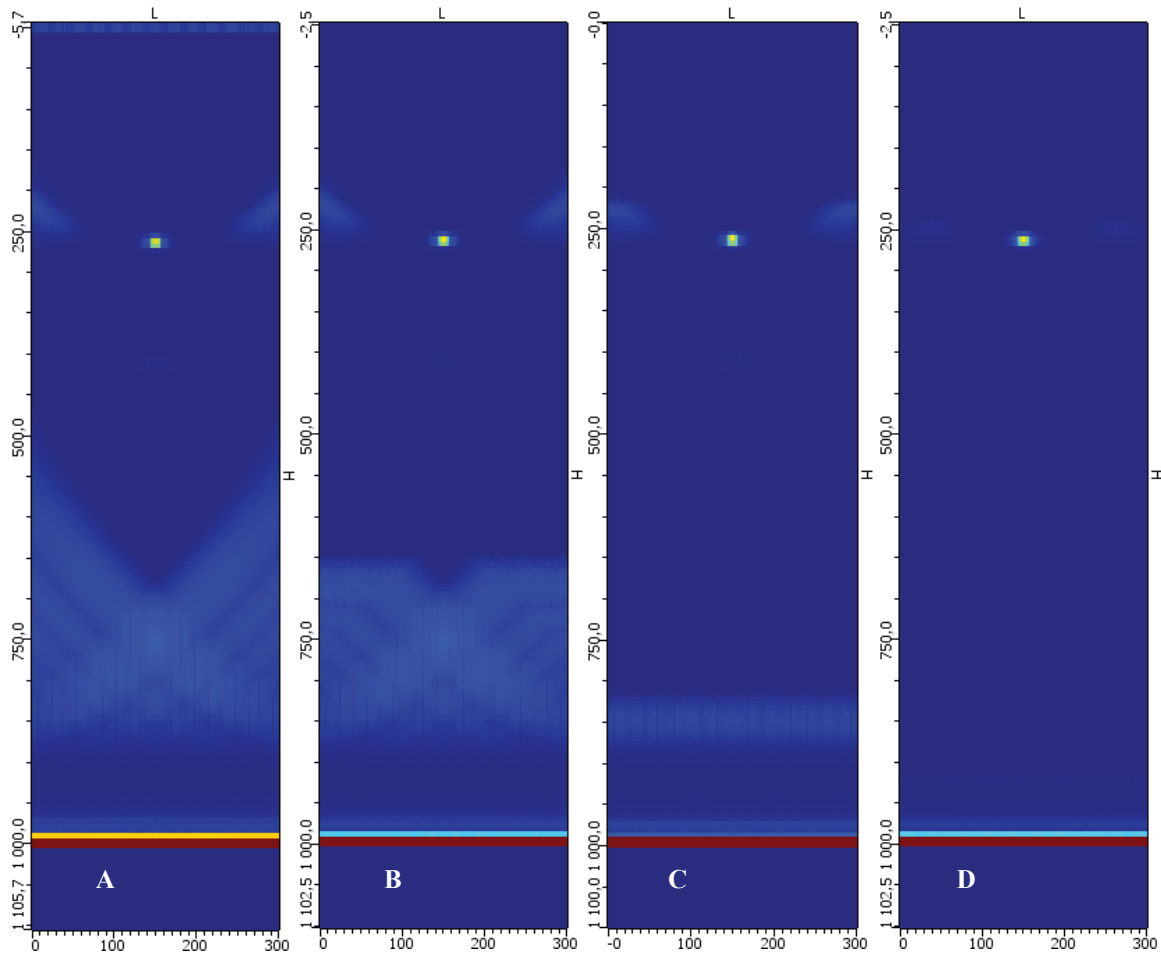


FIGURE 5. Large size forged steel imaging artefact removing using scattering cone filter from CIVA software: no filter (A), 40° (B), 30° (C) and 20° (D).

The scattering cone filter reduced artefacts but it also lowered the amplitude of the backwall and the defect. For this reason another method was proposed, and amplitudes were compared. The second method was based on the fact that the artefacts only appeared for a high element number, so the investigated solution was to cut FMC scan extreme sequences as a function of depth. All sequences near the surface were kept, whereas information from side sequences was cut for deeper regions. This principle can be observed for two defects at 265.5 mm and 900 mm with a 128 elements transducer.

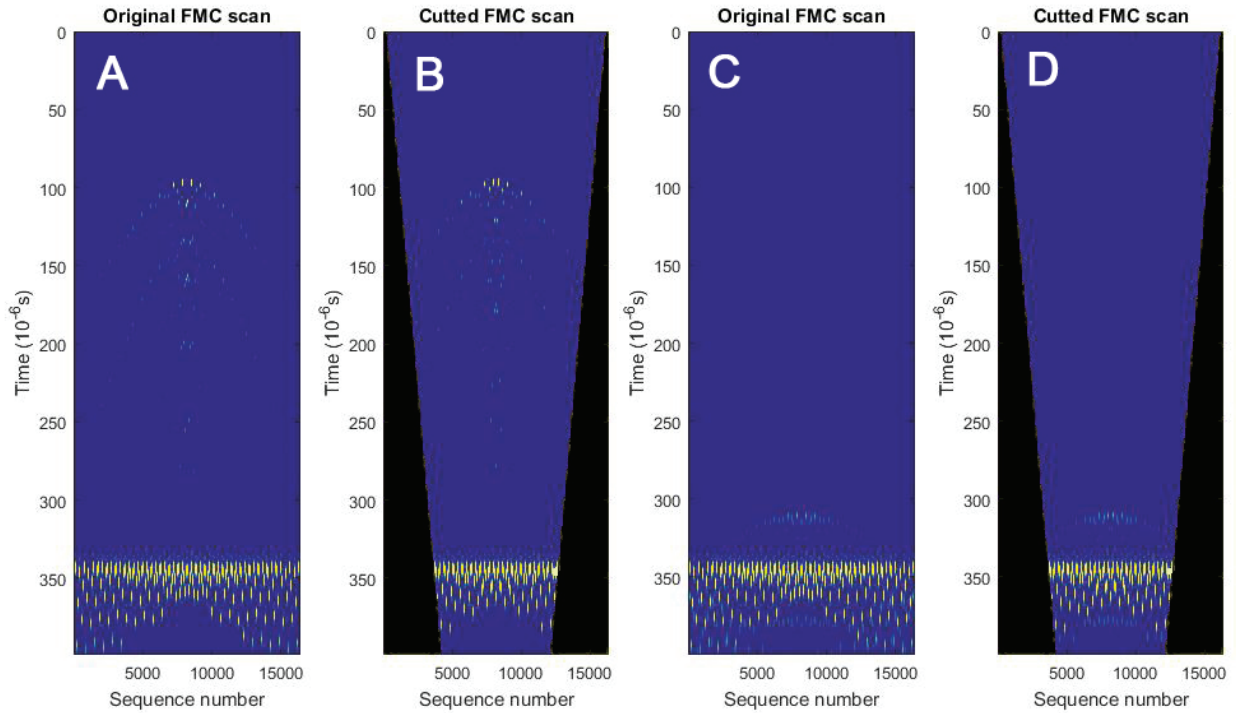


FIGURE 6. Full Matrix Capture removing sequences for artefacts removing in large size forged steel imaging using scattering cone filter from CIVA software: 265.5 mm depth defect (A and B), 900 mm depth defect (A and D).

With the TFM selection method shown in Fig. 6, the low depth resolution was not modified because the scans remain untouched. The TFM image reconstruction was then made using these FMC scans and results are presented in Fig. 7.

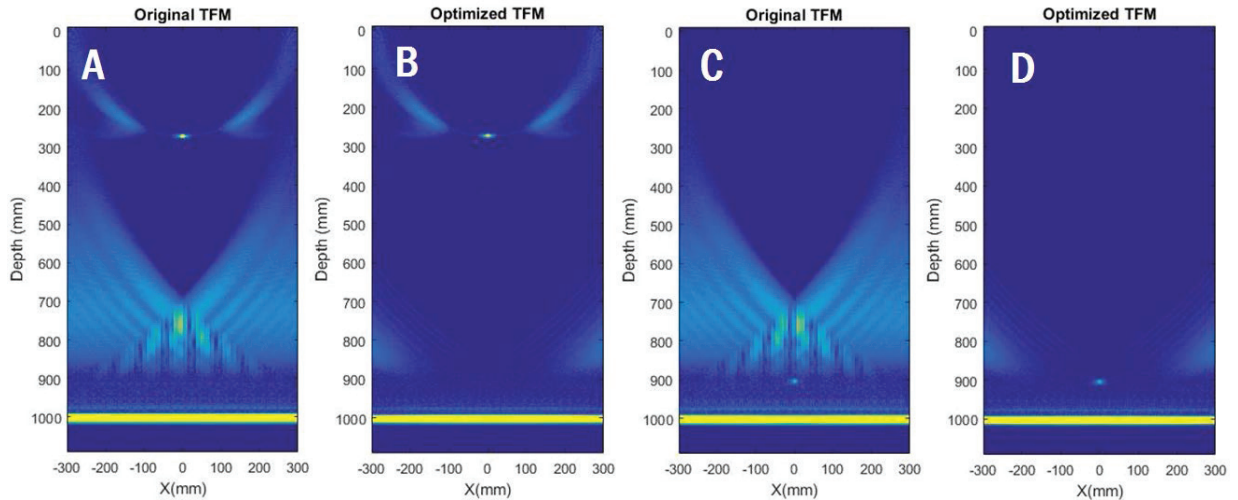


FIGURE 7. Full Matrix Capture removing sequences for artefacts removing in large size forged steel imaging using scan selection method: 265.5 mm depth defect (A and B), 900 mm depth defect (A and D).

Artefacts associated with backwall reflections were not totally removed on the sides of the TFM images. However in the central section of the image artefacts were suppressed and the defect was now clearly distinguishable. In order to quantify the reconstruction quality, the amplitudes of the two defects at 262.5 mm, 900 mm and the backwall were measured and compared with the one from scattering cone filter method. Results are given in Table 1.

TABLE 1. Amplitude comparison for artefacts filtering between the scattering cone filter method from CIVA software and the FMC scan selection method

angle	Amplitudes		
	Defect 262,5 mm	Defect 900 mm	Backwall 1000 mm
	Scattering cone filter method		
°	dB	dB	dB
no	-10,84	-42,57	0,00
40,00	-10,31	-41,99	0,00
30,00	-10,38	-42,57	0,00
20,00	-12,45	-46,25	-4,97
	FMC scan selection method		
	-10,84	-42,57	0,00

It was observed that the scattering cone filter method did not affect measurements for 40° and 30° cone angle, but it was also reducing defects and backwall amplitudes at any depth for a 20° angle. As observed previously in Fig. 5, artefacts were totally removed for a 20° angle and partially removed for a 30° angle. The scattering cone filter method requires a compromise between the amplitude loss that leads to less sensitivity and incomplete artefacts removal. On the other hand, FMC scan selection method provided superior results for suppressing artefacts along the vertical image centre axis, and it also kept defects and the backwall amplitude unmodified.

CONCLUSION

In this study, phased array inspection of large size forged steel was modelled in order to design a new transducer that would be adapted for the ultrasonic imaging of blocks with dimensions larger than 1000 mm in every direction. It was observed that standard probe with elements width in the region of 1 mm could not be used for the inspection of blocks that would be 400 mm or more. However, inspection was possible using wider elements, a design was determined, and its sensitivity and resolution were computed. It was found that a defect of 1.587 mm diameter at 400 mm would have an 18 dB loss from the reference backwall amplitude. The vertical and lateral resolutions would, respectively, be 5.5 mm and 25 mm. The second part of this study was focused on removing backwall artefacts that appeared for transducers designed with more than 64 elements with at least a 10 mm width. The scattering cone filter was compared with an FMC scan selection method. The scattering cone filter trades artefacts removal with a loss in sensitivity. The FMC scan selection method does not modify the amplitude of defects or the backwall and enables the suppression of artefacts along the vertical axis of the image.

REFERENCES

1. W. Gebhardt, F. Bonitz, and H. Woll, "Defect reconstruction and classification by phased arrays," *Materials Evaluation*, **40**:1, 90-95, (1982).
2. E. Iakovleva, S. Chatillon, P. Bredif, and S. Mahaut, "Multi-mode TFM imaging with artifacts filtering using CIVA UT forwards models," 40th Review of Progress in QNDE, *AIP Conf. Proc.*, **1581**, pp. 72-79, (2014).
3. P. Nanekar, A. Kumar, and T. Jayakumar, "SAFT-assisted sound beam focusing using phased arrays (PA-SAFT) for non-destructive evaluation," *Nondestructive Testing and Evaluation*, **30**:2, 105-123, (2015).
4. F. Foroozan and S. ShahbazPanahi, "Music-based array imaging in multi-modal ultrasonic non-destructive testing," *Sensor Array and Multichannel Signal Processing Workshop (SAM)*, pp. 529-532, (2012).
5. C. Fan, M. Caleap, M. Pan, and B. W. Drinkwater, "A comparison between ultrasonic array beamforming and super resolution imaging algorithms for non-destructive evaluation," *Ultrasonics*, **54**:7, 1842-1850, (2014).
6. A. Loucif, E. Ben Fredj, M. Jahazi, L.-P. Lapierre-Boire, R. Tremblay, and R. Beauvais, "Analysis of macrosegregation in large size forged ingot of high strength steel," *The 6th International Congress on the Science and Technology of Steelmaking (ICS2015)*, Beijing (China), (2015).
7. F. Dupont-Marillia, M. Jahazi, S. Lafreniere, and P. Belanger, "Influence of local mechanical properties of high strength steel from large size forged ingot on ultrasonic wave velocities," Review of Progress in Quantitative Nondestructive Evaluation (Vol. 36), *AIP Conf. Proc.*, **1806**, p. 090002, (2017).
8. J. D. N. Cheeke, "Fundamentals and applications of ultrasonic waves," CRC Press, p.452, (2012).
9. R. Long, J. Russell, and P. Cawley, "Ultrasonic phased array inspection using full matrix capture," *Insight - Non-Destructive Testing and Condition Monitoring*, **54**:7, 380-385, (2012).
10. C. Holmes, B. Drinkwater, and P. Wilcox, "The post-processing of ultrasonic array data using the total focusing method," *Insight-Non-Destructive Testing and Condition Monitoring*, **46**:11, 677-680, (2004).